



Morphological and Microstructural Characterization of Organoclays from Low Smectite Containing Clays Materials

Emeka Thompson Nwankwere^{1*}, Casimir Emmanuel Gimba²,
George Iloegbulam Ndukwe², Adamu Kari Isuwa³ and Yilleng Moses Titus⁴

¹Department of Physical Sciences, Kampala International University, Uganda.

²Department of Chemistry, Ahmadu Bello University, Zaria, Nigeria.

³Nigerian Institute of Leather Research and Technology, Zaria, Nigeria.

⁴Department of Chemistry, Kaduna State University, Kaduna, Nigeria.

Authors' contributions

This work was carried out in collaboration between all authors. All authors read and approved the final manuscript.

Article Information

DOI: 10.9734/CSJI/2017/29703

Editor(s):

(1) Yunjin Yao, School of Chemical Engineering, Hefei University of Technology, Tunxi, Hefei, Anhui, China.

Reviewers:

(1) Sunipa Roy, Guru Nanak Institute of Technology (JIS Grp), India.

(2) Renata Diniz, Federal University of Minas Gerais, Brazil.

(3) Nouha Jaafar, University of Carthage, Tunisia.

Complete Peer review History: <http://www.sciencedomain.org/review-history/17712>

Original Research Article

Received 24th September 2016
Accepted 4th January 2017
Published 3rd February 2017

ABSTRACT

Two low smectite-containing clay materials were modified, using hexadecyltrimethylammonium bromide (HDTMAB) as intercalating agents, under very mild experimental conditions, to investigate their potentials as suitable organoclays for industrial and environmental applications. Changes in the general morphological and microstructural characteristics were studied by X-Ray Diffraction (XRD) analysis, Thermogravimetric Analysis (TGA), Brauner Emmet Taylor (BET) Analysis, Fourier Transform Infrared (FTIR) Spectroscopy and Scanning Electron Microscopy (SEM) before and after modification. The shift in XRD reflections after intercalation indicated that the HDTMA chains adopt monolayer and bilayer arrangements within the clay interlayers and were largely dependent on the reaction time and surfactant loading. This resulted in decreased specific surface area and increased pore sizes in the organoclay samples. The presence of typical CH stretching bands in

*Corresponding author: E-mail: thompson.emeka@kiu.ac.ug, nemekathompson@yahoo.com;

the new materials was confirmed by FTIR analysis. Mass loss from TGA showed that the new materials were thermally stable, the amount of organic modifier in the organoclays were in good agreement with the theoretically calculated contents. The intercalated materials were hydrophobic, stable, biocompatible and were suitable materials for several industrial and environmental applications.

Keywords: Clays; HDTMAB; interlayers; organoclays; intercalation; smectites.

1. INTRODUCTION

The need to develop and study clay materials with notable properties and of useful applications such as environmental remediation [1–4], water purification [1,5,6], rheological additives [7–10], catalysis [11], food and agriculture [12–16], drugs [10,16–18] and nanohybrid precursors [19–22] has been on the rise over the past decade. Awareness and use of various types of clays and their beneficial effects can be traced down to the ancient Mesopotamians, Chinese, Indian and Egyptian civilizations to as far back as three to five hundred years ago [23]. Clays find a wide range of applications, in various areas of science due to their natural abundance and the propensity with which they can be chemically and physically modified to suit practical technological needs [24]. Clay is composed mainly of silica, alumina and water, frequently with appreciable quantities of iron, alkalis and alkali earths [25]. Clay minerals are natural environment-friendly materials with high specific surface areas and now widely used for the adsorption and removal of the organic pollutants [3,5,26–29]. They have been well known to mankind from the earliest days of civilization, with variability in their constitution depending on their groups and sources [18,25]. Clay minerals are essentially hydrous aluminosilicates with very fine particle sizes. Due to an isomorphous substitution within the layers, the clay mineral layer is negatively charged, which is counterbalanced by the exchangeable cations such as Na^+ , Ca^{2+} in the interlayers [30]. The hydration of the inorganic exchange ions present in clays and the nature of Si-O groups impart a hydrophilic nature to the mineral surfaces and this property makes them easy to absorb water but very difficult to disperse in organic matrices and hence renders the clay ineffective for interaction with aliphatic and relatively hydrophobic compounds [31,32]. The most studied methods for solving this problem generally involve the replacement of these exchangeable cations with an organic group. The process usually involves cation exchange with the surface and interlayer clay cations or a solid state reaction which usually involves an ion-

dipole interaction. The organic group is typically intercalated between the clay interlayer spaces and (or) adsorbed on the surface where the inorganic ions were previously attached. These types of modified clays are most often referred to as organoclays. In organoclay synthesis, the smectite clays are widely used, by virtue of their high cation exchange capacity, excellent ability to swell, high platelet aspect ratio and ease with which their surface can be modified [32,33]. Ion exchange with alkylammonium ions is the preferential method to prepare organoclays [9] and was employed in this study.

In this study, two natural clay materials with low smectite contents were selected, modified and investigated for their potential as suitable starting materials for organoclays. Low smectite-containing clays have an original low smectite content (ranging from near zero to approximately 15% smectite content). This work was aimed at modifying the materials by selective intercalation of their smectite compositions, under mild experimental conditions. How these modifications influenced some of the important properties of the materials were investigated. The synthesis of organoclays is dependent on the mechanisms of the reactions that the clay minerals can have with the organic compounds used. The effect of time and surfactant loading were specifically studied to give insight on the mechanism behind the transformation and also to address how the materials changed in their properties and morphology when exposed to hexadecyltrimethylammonium (HDTMAB) bromide, a popular intercalant in clay science.

2. MATERIALS AND METHODS

Two natural low smectite-containing clay samples sourced within Nigeria [Adamawa (9°33'N 12°43'E) and Yobe (12°00'N 11°30'E) States], coded Sample A and Sample C respectively, were collected from the National Geosciences Research Laboratory, Kaduna, Nigeria. All samples were pulverized, sieved (<200 μm), and stored in dry plastic bags prior to modification. HDTMA bromide (Sigma-Aldrich)

was used to carry out the cation exchange reaction in the synthesis of the organoclays using the simple hydrothermal method [30,31], under very mild reaction conditions.

Prior to hydrothermal modification, the clay samples were purified using the synthetic methods described in Pedro et al., [34], where the clay samples were first dispersed in distilled water to separate unwanted fractions by sedimentation and filtration based on Stokes' law of settling in suspension. The collected samples, like with most raw clays contained a mixture of several mineral phases as impurities. Smectites, like most clay minerals, by their very nature, are extremely fine grained, and it is this attribute that is utilized to separate them from more coarse-grained minerals with which they commonly coexist (quartz, feldspar, calcite and other impurities). The dispersed clay samples were collected and treated with Dithionite-Citrate-Bicarbonate (DCB) to remove all iron oxide and hydroxide in the clay suspension. The DCB solution was removed by centrifugation and the clay samples washed severally until pH was 7. The treated clay samples were finally treated with hydrogen peroxide and sodium acetate solution to remove organic substances from the clay as explained in Manocha et al. [31]. The treated samples were dried at 105°C and labelled as Sample 1 and Sample 3 for Sample A and Sample C respectively.

For Intercalation experiments, the treated samples (Sample 1 and Sample 3) were placed in separate 200 ml beakers and heated in a water bath until they reached the desired temperature. To the samples in the beakers, selected concentrations based on the CEC of the salt sample were added. The mixture was stirred until it reached the desired time for the hydrothermal process to complete. The samples were then removed from the beaker and centrifuged and washed with hot distilled water until all loose Br atoms were removed from the organoclay solution. This was confirmed using AgNO₃ test, as no precipitates were formed in the collected supernatant solution. The centrifuged organoclay was dried in the oven at 85°C, pulverized, sieved below 200 µm and then kept in a desiccator for subsequent experimentation. The procedure was repeated by varying the time (2.5, 5, 7.5, 10 and 12.5 hours), on Sample A and by varying the surfactant concentrations (5, 10, 20, 30, 40 and 50 percent w/w material) on Sample C.

The Cation Exchange Capacity (CEC) of the raw and purified clay materials were determined using the barium chloride compulsive exchange method [35]. The surface area, porosity and pore sizes of the clays and their corresponding HDTMA organoclays were measured from N₂ sorption isotherm at 77 K using a Micrometrics Tristar II BET analyser. The samples were degassed under flowing nitrogen at 250°C for 4 hours using the Smart Prep™ 065. The degassing unit removes adsorbed contaminants from the surface and pores of a sample in preparation for Brauner Emmet Taylor (BET) analysis. The chemical compositions of the clay minerals before and after modification were measured by X-ray fluorescence spectroscopy (XRF) using an Oxford Instrument (X-supreme 8000) with a tungsten X-ray tube and powder sample holder. Concentrations were expressed in percentages (%).

X-Ray Diffraction (XRD) analysis gives information about the interlayer spacing of the materials which is very important for explaining the intercalation and configuration of organic surfactant into the material and also enables the determination of the expansion as well the crystal size of the clay [36]. X-ray Diffractometer (XPRT-PRO, PW3064, Copper K α radiation at 40 kV/40 mA, with a goniometer velocity of 2°/min and a step of 0.05°, with 2 θ ranging from 0° to 89°) was used to probe the crystal lattice structure and interlayer space of the clay and organoclay powders. To determine whether a chemical reaction took place between organic compounds and the clay samples and also to investigate the position, manner of arrangement and presence of characteristic organic groups in the sample's structure, Fourier Transform Infrared (FTIR) analysis was carried out. FTIR characterization has been proven to be an effective method for exploring the microstructures of organoclays [37–40]. The FTIR spectra were recorded on a Shimadzu FTIR-8400s Spectrophotometer using KBr, with 20 scans collected for each measurement over the spectral range of 4000-400 cm⁻¹ with a resolution of 4 cm⁻¹. Each sample (2.0 mg) was mixed thoroughly with 150 mg of spectroscopic grade KBr and dried in an oven at 120°C for about 12 hours before analyses. All spectra were presented without baseline correction or normalization. Since FTIR spectroscopy measures the molecular vibrations and determines the molecular structure of the organoclays, any change in the structure of the

organoclay will be observed through alterations in the infrared spectra [17,36].

To determine the surface morphology before and after modification, Scanning Electron Microscopy (SEM) was carried out using a Phenom™ X-pro Scanner, with 5 KV of accelerating voltage. The samples were sputter coated with thin conductive layer gold before analysis. Thermogravimetric Analysis (TGA) and Differential Thermal Analysis (DTA) were used to investigate the thermal and energy profile of the clay and organoclays materials. Thermal studies play an essential role in determining both technological applications and processing conditions of the clay materials and can lead to new insights into the structure of the intercalated clay [37,41]. A Mettler-Toledo TGA/DSC1 Star® (Mettler-2012) instrument with a heating rate of 20°C/min in Nitrogen (N₂) atmosphere was employed in determining the thermal characteristics of the raw and modified clay samples. All of the samples were heated up to 500°C.

3. RESULTS

3.1 Analysis of Surface Properties and Morphology

N₂ adsorption data from BET analysis used to investigate the surface properties of the materials are presented in Table 1. Decreased values in the pore volumes and SA_{BET} of the samples were observed after modification. The observed reduction in the pore volume of Sample A and Sample C from 0.054 and 0.053 cm³/g respectively to 0.017 cm³/g after modification are due to the organic molecules filled in the clay interlayers. Carmody et al. [42] observed that drying materials may result in a significant and irreversible reduction in pore volumes and hence resulting to the internal SA of the materials being inaccessible to N₂ molecules. The measured specific surface areas of clay minerals are the sum of the surface areas of the interspaces (micropores), the intraparticle spaces (micro/mesopores inside the assembly of the silicate layers), and the inter-aggregate spaces (meso/micropores inside the assembly of particles [43,44]. The SA_{BET} of Sample A and Sample C which were 18.256 m²/g and 47.728 m²/g were also reduced to 5.113 and 5.323 m²/g in Samples 2 and 5 respectively. The decreased surface area of the organoclay samples, with respect to the values of their corresponding raw clay samples, is a consequence of the disappearance of micropores, which is caused by

the blocking of the N₂ passage by the large HDMA cations in the clay interlayer, leaving only a small fraction of the interlamellar pores accessible [44,45]. The decrease in SA_{BET} of the organoclays largely depends on the packing density which may be predominantly occupied by long-chain HDMA⁺ in the interlamellar layer resulting in more serious pore blocking that inhibits the passage and adsorption of N₂ in the organoclay [42,46,47,48], since the HDTMA cations were too strongly bound to be physically replaced by N₂ molecules. These findings suggest that the HDTMA cations are introduced inside the interlayer of the clay mineral not only by cation exchange at the planar sites but also through the interaction with the aluminosilicate sheets [48,49]. The surface areas of the organoclays and raw clay samples are interrelated at the level of stacking of elementary layers in that the adsorption by reaction with the planar sites and the consequent formation of outer-sphere complexes is likely to occur [50]. Higher surface area of raw clay samples in comparison to that of their respective organoclay samples suggests that the latter samples may have a considerable amount of the trapped pores in the range of small and medium mesopores (20–400 Å). The amount of the trapped pores in the raw samples are lower than those of their corresponding organoclays which can be explained by the development of larger mesopores as a result of the arrangement of HDTMA cations in the interlayer spaces of these samples. IUPAC recommendation for pores are classified as <2nm for micropores, 2nm<size<50nm for mesopores and >50nm for macropores. The average pore sizes of the samples showed that they were mainly mesoporous and had increased from 124.392 (Sample A) and 58.355 Å (Sample C) in the raw samples to 137.396 (Sample 2) and 148.449 Å (Sample 5) respectively, along with the observable decrease in pore volumes. Increased pore sizes suggested that the surfactants were intercalated into the interlayer spaces of the clays rather than being adsorbed/precipitated to/in interparticles and aggregate species. The insertion of HDMA⁺ cations, by the exchange process, into the raw clays, increased the number of medium and large mesopores and caused the significant decrease in the surface areas and pore volumes of the organoclays compared to the raw samples. The results indicated that the exchanged cations affect the surface characteristics of the clays in some manner that appears to be related to the size and interlayer arrangement of the exchanged ion in

the material samples [48]. These results are similar to the findings of other researchers [44] indicating that the materials can sufficiently be applied as functional organoclays.

3.2 Analysis of Crystal Structures by XRD

The characteristic d001 smectite reflections of the raw and the modified clay materials studied by XRD were summarized in Table 1. Reflections corresponding to the 001 reflections of smectite

minerals at 2θ positions of approximately $7^\circ 2\theta$ or 12.5 \AA were clearly indicated. Reflections relating to the presence of other mineral phases were an indication that the purification procedure was not absolute for the samples employed. In the diffractograms of Samples A and B, the characteristic reflections were at $7.6^\circ 2\theta$ and $5.8^\circ 2\theta$, which also correspond to interlayer spaces of 11.5 \AA and 15.3 \AA respectively. The effects of reaction time and surfactant dosage were also studied and are illustrated in Fig. 1 and Fig. 2.

Table 1. Summary of the properties of the tested clays and organoclay samples

| Properties | Raw clay samples | | Purified clay samples | | Organoclay samples | |
|---------------------------------------|------------------|----------|-----------------------|-----------------|--------------------|-----------------|
| | Sample A | Sample C | Sample 1 | Sample 3 | Sample 2 | Sample 5 |
| Modified from | | | Sample A | Sample C | Sample A | Sample C |
| Al ₂ O ₃ (%) | 29.141 | 25.797 | 32.324 | 28.43 | 39.353 | 27.638 |
| SiO ₂ (%) | 65.538 | 53.002 | 60.8 | 57.84 | 54.093 | 55.692 |
| TiO ₂ (%) | 2.211 | 1.52 | 1.29 | 2.45 | 2.789 | 1.659 |
| Na ₂ O (%) | 0.077 | 2.959 | 1.26 | 1.63 | 0 | 0.516 |
| MgO (%) | 0.523 | 1.831 | 1.043 | 1.429 | 0.616 | 1.574 |
| Fe ₂ O ₃ (%) | 1.318 | 12.124 | 1.112 | 7.142 | 2.361 | 11.207 |
| MC (%) | 0.40 | 3.27 | 0.64 | 1.42 | 0.00 | 0.00 |
| OMC (%) | 0.00 | 4.00 | 0.00 | 1.04 | 24.00 | 16.00 |
| Pore Volume (cm ³ /g) | 0.054 | 0.053 | 0.062 | 0.054 | 0.017 | 0.017 |
| Pore Size (Å) | 124.392 | 58.355 | 103.121 | 58.654 | 137.396 | 148.449 |
| SA _{BET} (m ² /g) | 18.26 | 47.73 | 22.23 | 46.43 | 5.113 | 5.323 |
| CEC (Meq/ g) | 98.24 | 92.6 | 102.32 | 100.24 | - | - |
| d001 (Å) | 11.6 | 15.3 | 11.6 | 15.4 | 20.3 | 17.9 |

MC stands for moisture content; OMC, Organic matter content; SA_{BET}, Bruner Emmet Teller Specific Surface Area; CEC, cation exchange capacity; and OC stands for the Organoclay samples tested

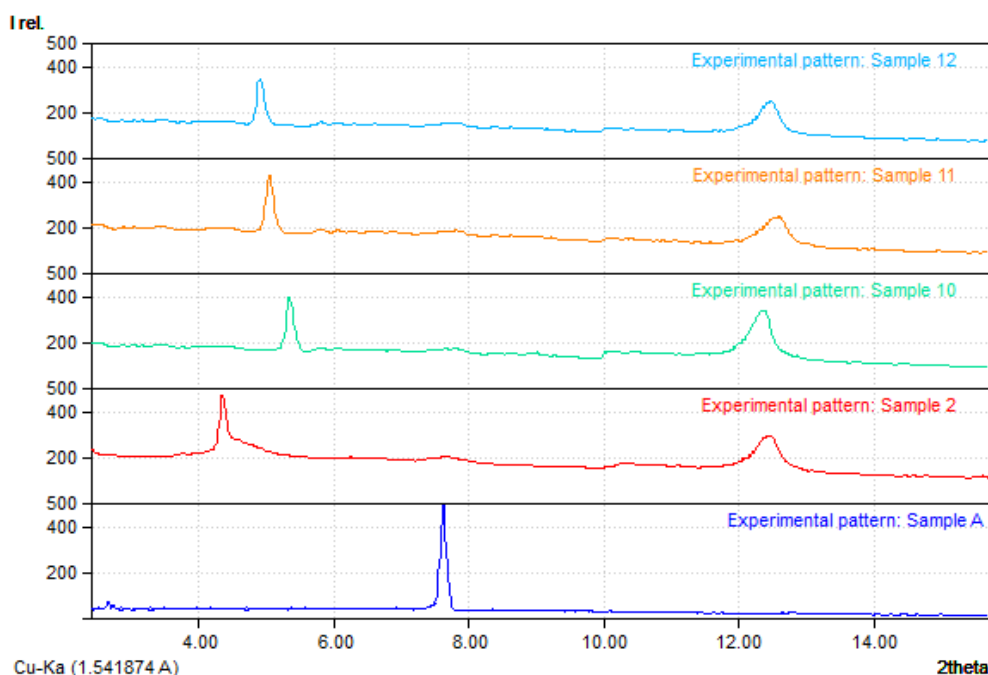


Fig. 1. The effect of time on intercalation: XRD diffractograms of samples A, 2, 10, 11 and 13

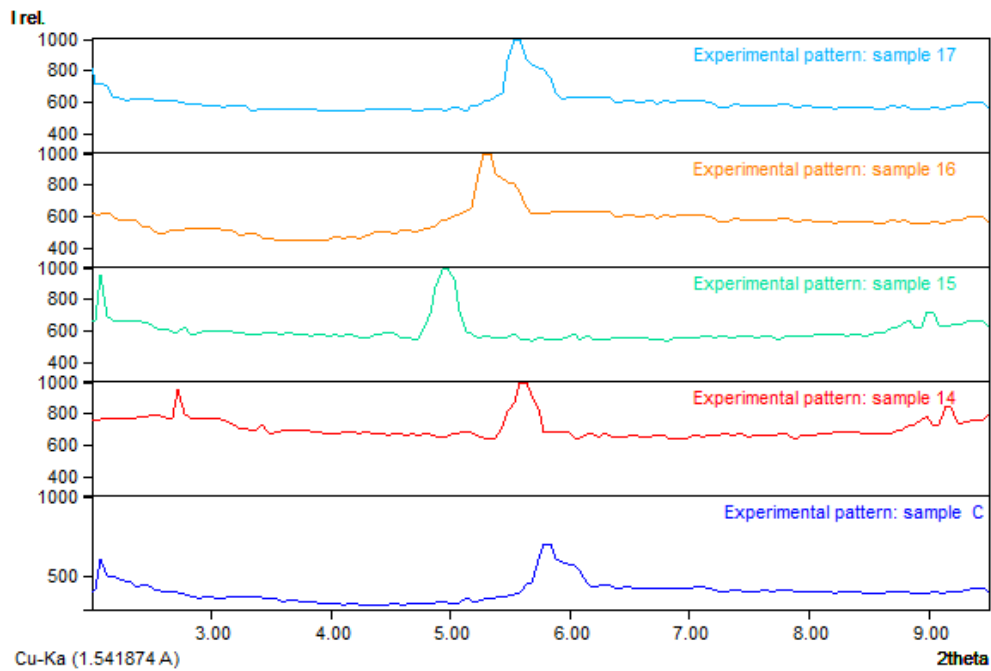


Fig. 2. The effect of surfactant concentration on intercalation: XRD patterns of Samples C, 5, 14, 14, 15 and 17

Table 1. The effect of reaction time and surfactant concentration on intercalation

| S/N | Sample ID | Modification conditions | | | Reflection | |
|-----|-----------|-------------------------|------------|----------|------------|------|
| | | Temp (°C) | Time (Hrs) | Conc (%) | °2θ | Å |
| 1 | Sample 2 | 80 | 10.0 | 50 | 4.4 | 20.3 |
| 2 | Sample 10 | 80 | 2.5 | 50 | 5.4 | 16.5 |
| 3 | Sample 11 | 80 | 5.0 | 50 | 5.0 | 17.5 |
| 4 | Sample 12 | 80 | 7.5 | 50 | 4.9 | 18.1 |
| 5 | Sample 13 | 80 | 12.5 | 50 | 4.5 | 19.6 |
| 6 | Sample 5 | 80 | 10.0 | 50 | 5.2 | 17.1 |
| 7 | Sample 14 | 80 | 10.0 | 30 | 5.6 | 15.8 |
| 8 | Sample 15 | 80 | 10.0 | 20 | 5.0 | 17.9 |
| 9 | Sample 16 | 80 | 10.0 | 10 | 5.3 | 16.6 |
| 10 | Sample 17 | 80 | 10.0 | 5 | 5.6 | 15.9 |

Sample ID represents the sample number for each of the examined organoclays; T(°C) represents the Temperature (in °C); Time (hrs) represents the interaction time (in hours); Conc is the concentration of the surfactant used; and Å is the characteristic d001 smectite interlayer space of the materials in Å

After intercalation, the reflections shifted leftward from this first characteristic reflection towards lower angles, indicating an increase in the interlayer space of the materials. The clay sheets were bound with in-plane covalent bonds and therefore their crystal structures were stable. The change in the crystal structure was indicative of the expansion of the interlayers by the alkylammonium ion. The interlayer space of alkylammonium clays changes in a characteristic way with the length of the alkylammonium [9]. Clay mineral layers are held loosely with Van der Waals bonds and hence expansion of interlayers

is commonly seen when water or organic molecules are introduced between the layers [39]. The layers of the clays were propped open upon swelling in water in the presence of the alkylammonium surfactant. After the ion exchange process, the cationic head groups of the intercalation agent molecule would preferentially reside at the layer surface and the aliphatic tail will radiate away from the surface expanding the d-value in comparison with that of the original clay sample [36,37]. This is a characteristic property of smectites.

Although exchange reaction were quite fast (about 40–120 min), Nguyen et al. [51] suggested that in order for cations to be stable between clay mineral layers, reaction solution should be kept in longer time. The modification process, carried out at 80°C using 50% wt. HDTMA was repeated for 2.5, 5, 7.5, 10 and 12.5 hours. An evident increase in interlayer space with increasing time from 11.5 Å for Sample A to 20.3, 16.5, 17.5, 18.1, and 19.6 Å for the modified Samples 2, 10, 11, 12 and 13 respectively were shown in Fig. 1. The modification process induced noticeable effects on interlayer space after the first 2.5 hours (16.52 Å), and the maximum interlayer space (20.3 Å) was obtained after 10 hours. No further increase in spacing was observed after the 10-hour process. Instead, there was a decrease in the interlayer space to 19.6 Å when the process was allowed to stay for 12.5 hours. The shift of the XRD reflections as time progressed can be attributed to re-orientation of the long organic salt chain between MMT layers into more condensed configurations [52,53].

XRD reflections of the modified materials, in Fig. 2, shifted to new positions with an increase in surfactant loading confirming that intercalation and surface modification of Sample C had taken place. Upon increasing the concentration of HDTMA additional increase in spacing was observed. The interlayer space increased from 15.3 Å to 19.6 Å, 15.8 Å, 17.9 Å, 16.6 Å and 15.9 Å, in response to increase in the surfactant concentration from 5% to 50%, 30%, 20%, 10% and 5% respectively. However, little effect was observed in the change of the d001 values from 15.3 Å in Sample C to 15.9 Å in Sample 17 (5% HDTMA). The increments in interlayer spaces were highly dependent on the concentration of the surfactant used and were attributed to the intercalation of cationic surfactant into the interlayer spaces.

The reflections of the effect of reaction time and the effect of concentration fall between 15.00 and 20.00 Å indicating HDTMA chains adopt monolayer (13.7 – 17.5 Å) and bilayer (17.7 – 21.7 Å) arrangements of in the layers of the smectite sheets [41,52,54,55], which is in contrast to the predicted pseudotrimolecular arrangement when the number of carbons on the tail group of n-alkylammonium is sixteen [52,56]. The results agree with the measured interlayer spaces of HDTMA intercalated bentonites (14.0 to 18.0 Å) [57] with monolayer and bilayer configurations.

3.3 Analysis of Microstructural and Chemical Properties by FTIR Analysis

The FTIR spectra of the clay samples and their resultant organoclays, within the range of 4000 to 400 cm^{-1} , are shown in Fig. 2 and Fig. 3. The infrared spectra of the unmodified clays, Sample A and Sample C, showed major bands that are characteristic of smectite clay minerals. Bands in the 600-400 cm^{-1} region were attributed to Si-O and Al-O bending bands with interlayer deformation around 1630 cm^{-1} . The tetrahedral bending modes were near 430 cm^{-1} for Si-O-Si and 540 for Si-O-Al [58]. Si-O bending modes was observed at 790 and 690 cm^{-1} indicating the presence of quartz in the materials [25]. The intense broad bands observed between 1100 and 1020 cm^{-1} were those for also Si-O stretching bands of the smectites. The band in the 3600-3440 cm^{-1} region were ascribed to OH stretching of hydroxyl groups present in the interlayer of the clay material by covalent attachment to the silane molecules. The spectra showed prominent bands between 3622 and 3695 cm^{-1} indicating the possibility of hydroxyl linkage due to OH stretching band of structural OH group from Al-Al-OH and Si-OH-Al stretching (interlayer) with the bending mode at 914 cm^{-1} (and 922 cm^{-1}), which are the characteristics of dioctahedral smectites.

Common features in the spectra of the organoclays were the appearance of band wavenumbers around 3655 cm^{-1} , 2852 cm^{-1} , 2922 cm^{-1} , 1470 cm^{-1} , 1010 cm^{-1} , 752 cm^{-1} and 432 cm^{-1} . The organoclays do not only have characteristic smectite bands but also have characteristic alkyl or aryl group bands. The FTIR spectra of the organoclays showing the effect of time and ammonium salt concentration are also observed in Fig. 2 and Fig. 3 respectively. In the spectra of the organoclays, bands in the 3700-3300 cm^{-1} region were attributed to the O-H dimers present in the raw minerals. By cation exchange, HDTMA⁺ was intercalated into the interlayers of the clay materials, broadening the absorption bands origins. This resulted to the transformation of the surface properties from hydrophilic to hydrophobic and to the replacement of the hydrated interlayer cation with those of the surfactant. The difference in the absorption bands of the Mg-Al-OH band for the organoclays and those of the raw clays were attributed to the relaxation of hydrogen bonding between Al-Mg-OH as well as the hydrated water of exchangeable cationic metal ions in the clay surface [39].

The IR bands that appeared in the 3000-2800 cm^{-1} region were the signatures of CH_2 infrared absorption bands. These bands are indicative of the ordering (gauche/trans conformer ratio), packing density of the surfactants in organoclays and the interactions between the alkyl chains [40]. The bands at 2922 cm^{-1} were also due to asymmetric C-H stretching band of CH_2 aliphatic and the absorption bands at 2852 cm^{-1} corresponds to symmetrical CH_3 stretching [59]. The presence of CH_3 and CH_2 transmission bands in organoclays confirmed intercalation while the systematic decrease or weakening of intensity of OH (free) stretching bands confirmed that the materials became more and more hydrophobic with increasing alkylammonium ion concentrations. According to previous reports [29,41,60–62], the CH_2 infrared absorption bands on FTIR patterns, especially the ν_{as} (CH_2) mode, are sensitive to the packing density of the adsorbed surfactants on clays, and the absorption frequencies of ν_{as} (CH_2) are believed to be inversely related to the packing density of the adsorbed surfactants [40]. It is evident that there was a shift for these bands towards lower wavenumbers as the surfactant loading rate increased from 25% to 70% (w/w). The results supported the evidence from the XRD results, that increasing surfactant packing density causes additional expansion of the clay interlayer spaces. The results of this study agree with the findings of Zhu et al. [40] and are attributed to the progressively developing conformation of the

adsorbed surfactant molecules from low packing density and ordering (liquid like) to high packing density and ordering (solid like). Bands due to asymmetric and symmetric modes did not appear in the case of unmodified clays due to the absence of organic molecules therein. The peaks at 1660 - 1620 cm^{-1} were due to H-O-H bending band and the intensity reflected the amount of water in the interlayer [52]. The IR absorption band around 1480 cm^{-1} is normally ascribed to the antisymmetric angular deformation or bending mode of the head ($(\text{CH}_3)_3\text{N}^+$) methyl group of the HDTMA⁺ and has been noted to be sensitive to the extent of disorder and packing of the head group [28,52].

3.4 Analysis of Microstructural Properties by SEM

Fig. 5 to Fig. 8 show the SEM images of the clay samples before and after modification. The original samples (Samples A and C) had massive, curved plates and bulky flakes with aggregated morphology. On the other hand, the modified samples (Samples 2 and 5) were discrete and gathered together much easier than those of the raw samples. They were characterized by several small and scattered platelets that are relatively flat. The modified samples showed a more heterogeneous agglomeration in terms of dimension and particle size (polydispersity), comprising many irregular lamellae very likely because of the interactions

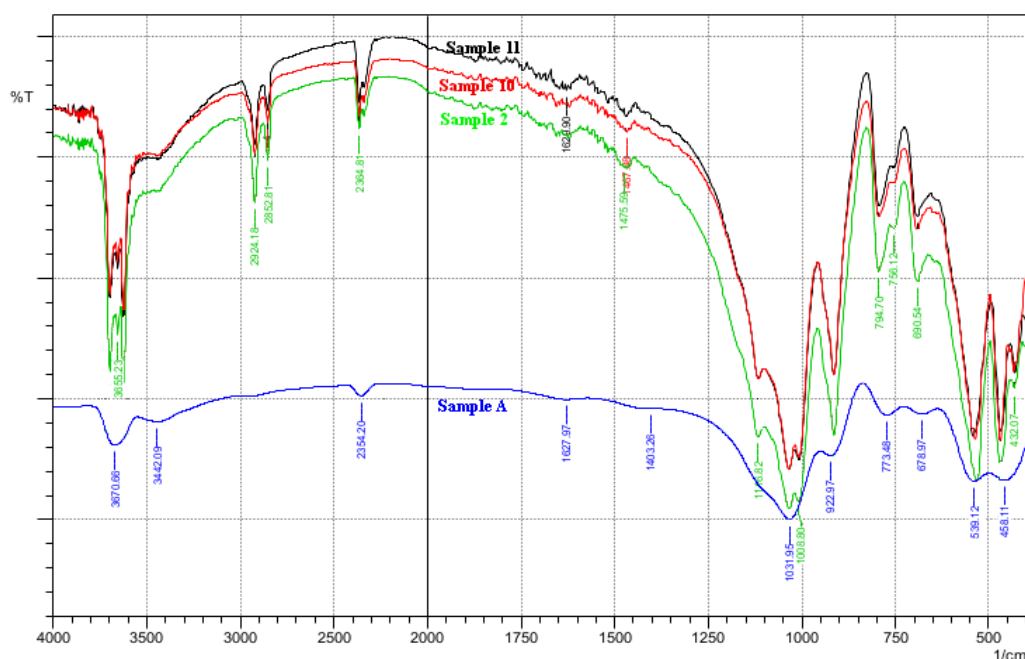


Fig. 3. FTIR spectra of samples A, 2, 10 and 11

between the alkyl groups of surface exchanged molecules belonging to different particles. The scattered platelets imply an increase in the interplanar distance by the presence of the intercalated alkylammonium ions that tends to transform into local clusters with a high packing density. It is also of importance to reveal that although the organoclay materials showed a

significant change in morphology compared to their original nature, there were not many morphologic differences observed despite the obvious variation observed in the XRD and FTIR measurements. The retention of some characteristic properties of the natural clay materials after giving the chemical treatment can be distinctly observed.

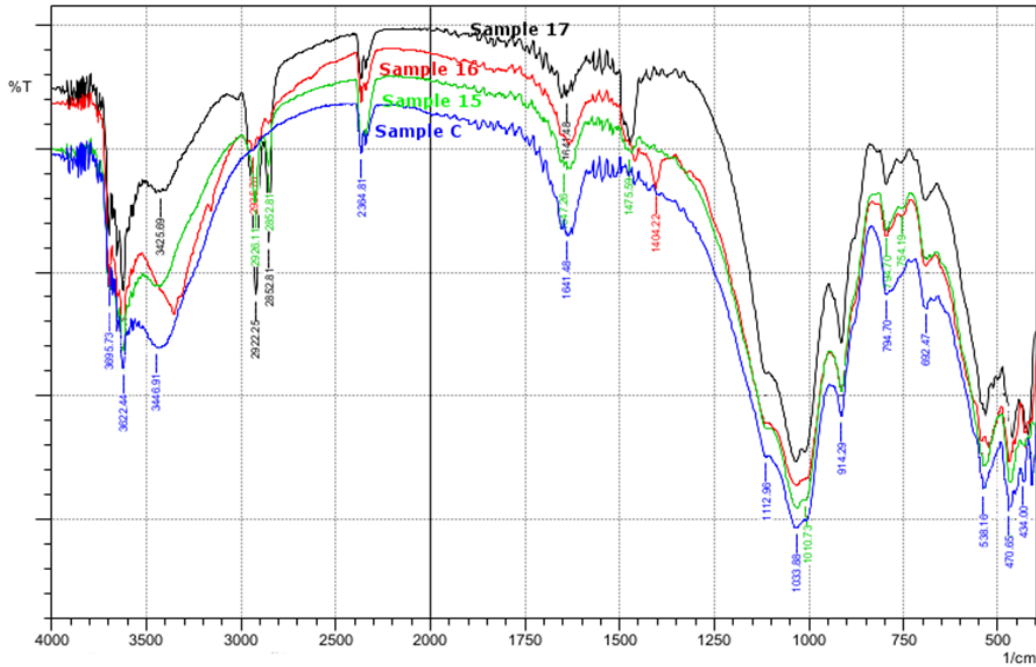


Fig. 4. FTIR spectra of samples C, 15, 16 and 17

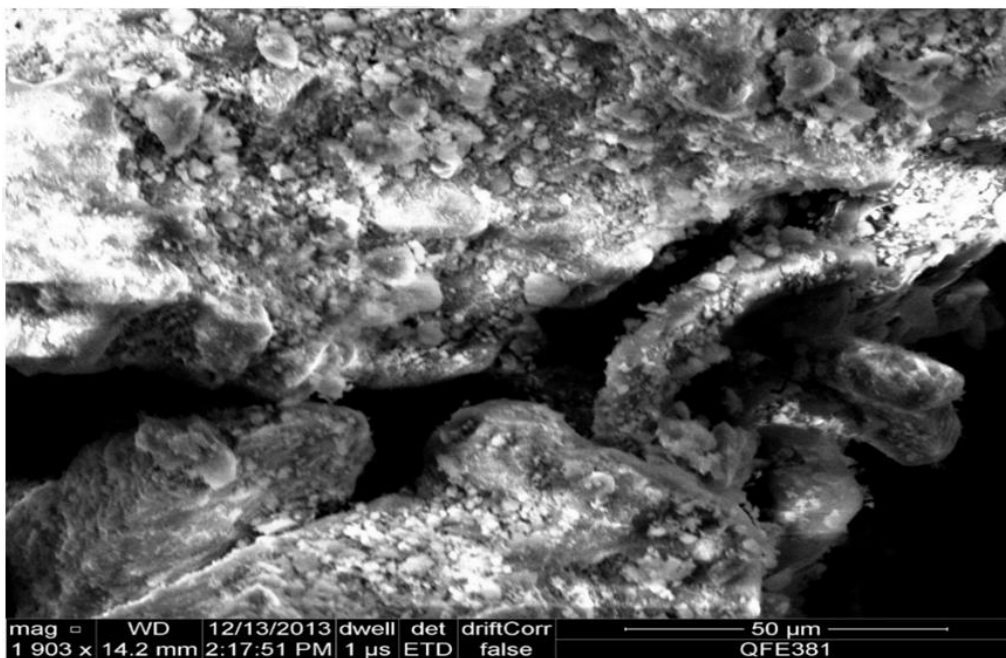


Fig. 5. SEM micrograph of sample A

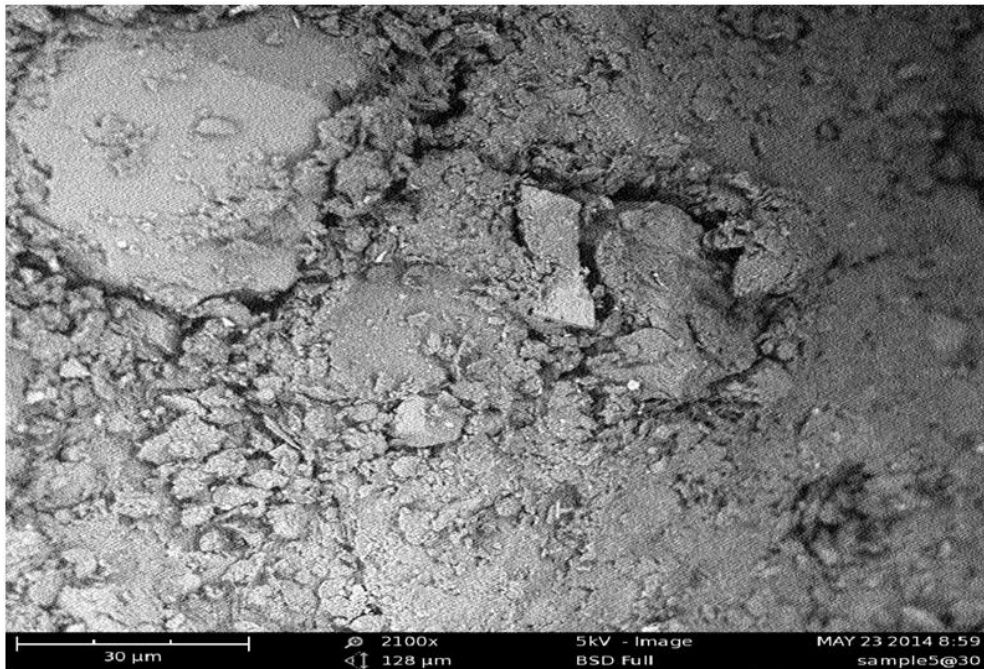


Fig. 6. SEM micrograph of sample 2

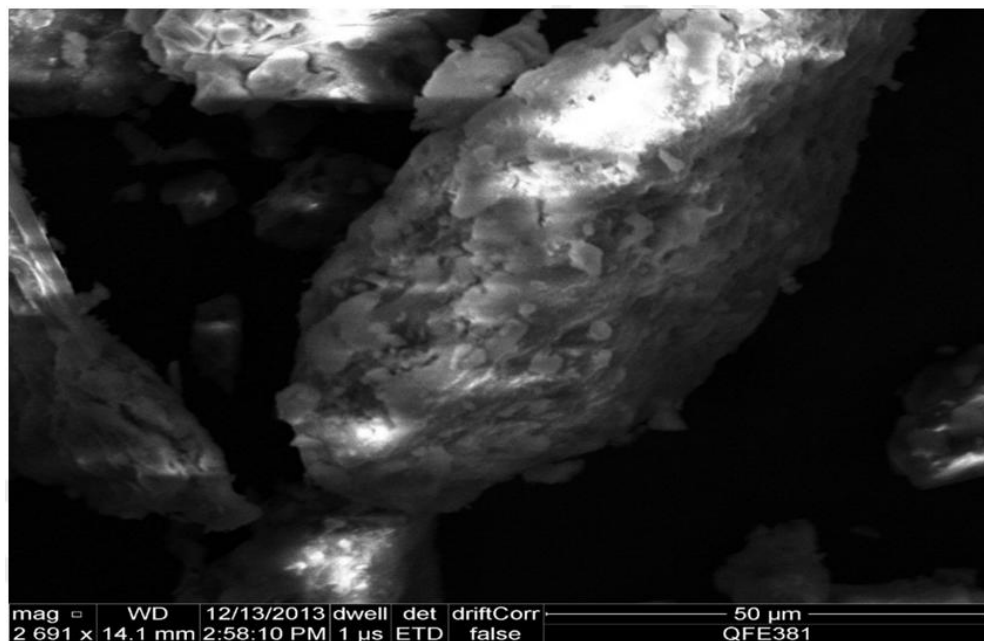


Fig. 7. SEM micrograph of sample C

3.5 Thermoanalytical Characterization and Degradation Behaviour

The TGA and DTG profiles of the raw and modified samples are shown in Fig. 8 to Fig. 11. Fig. 8 and Fig. 9 display the results of the raw clay samples while Fig. 10 and Fig. 11 display those of the modified samples.

At a given temperature the clays' and organoclays' mass losses are directly related to the rate of the material decomposition process [37]. The way in which the mass loss steps occur provides information on the properties of the inserting molecules. This study explains a four step mass loss covering 50 to 500°C to enable a better understanding of the sample characteristics.

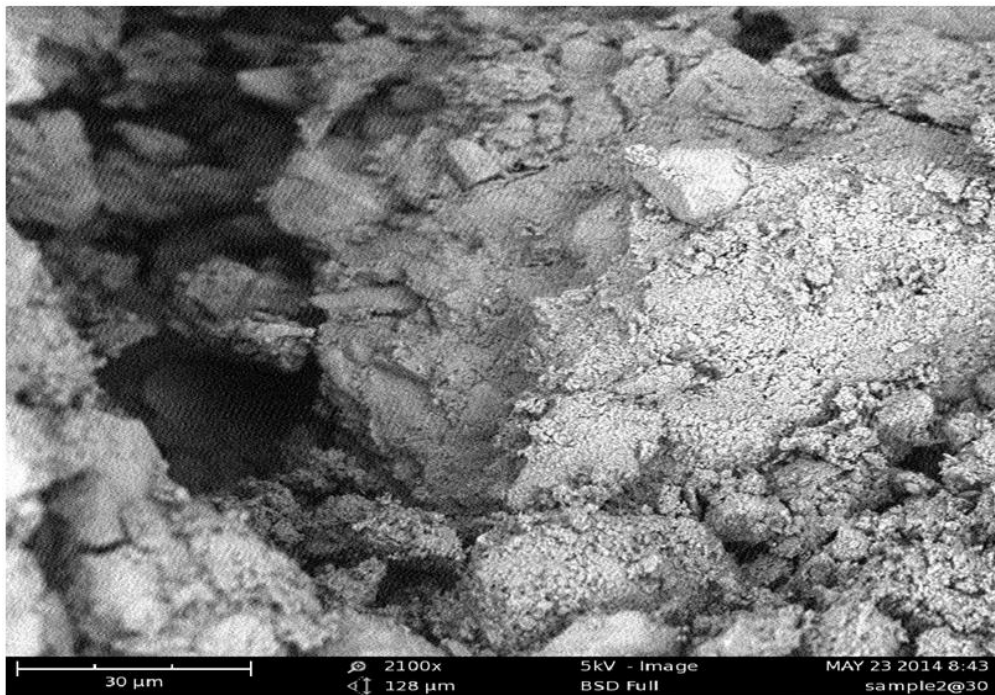


Fig. 8. SEM micrograph of sample 5

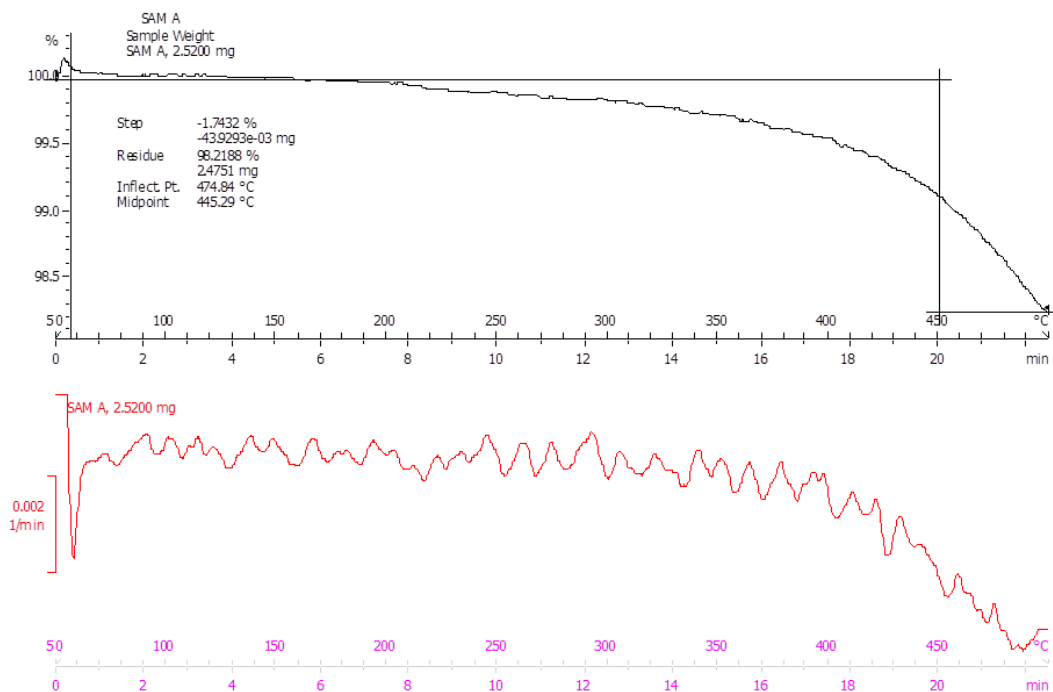


Fig. 9. Thermogram of sample A

The first step forms the ambient to 110°C temperature range and is attributed to desorption of water from the clay [63]. Free water (water between particles and adsorbed on the external surfaces of crystals) are released at temperatures of below 110°C. This explains the

hydrophobic character and at the same time the moisture contents of the materials. The thermogram recorded an initial sample mass of 2.52 mg for Sample A which did not show any major decrease in the first 110°C. Sample C decreased in mass by about 3.27% (0.28 mg)

from an initial sample mass of 8.46 mg. The DTG of Samples C shows a deep broad trough with a maximum at 90°C. This indicates that the raw samples were not thermally stable within the first step. This was only possible due to the loss of physisorbed and chemisorbed water [64]. In the

organoclay samples, the initial masses of Samples 2 and 5 were 7.98 mg 4.93 mg respectively. There were no obvious changes in the masses of Samples 2 and 5 from the thermograms.

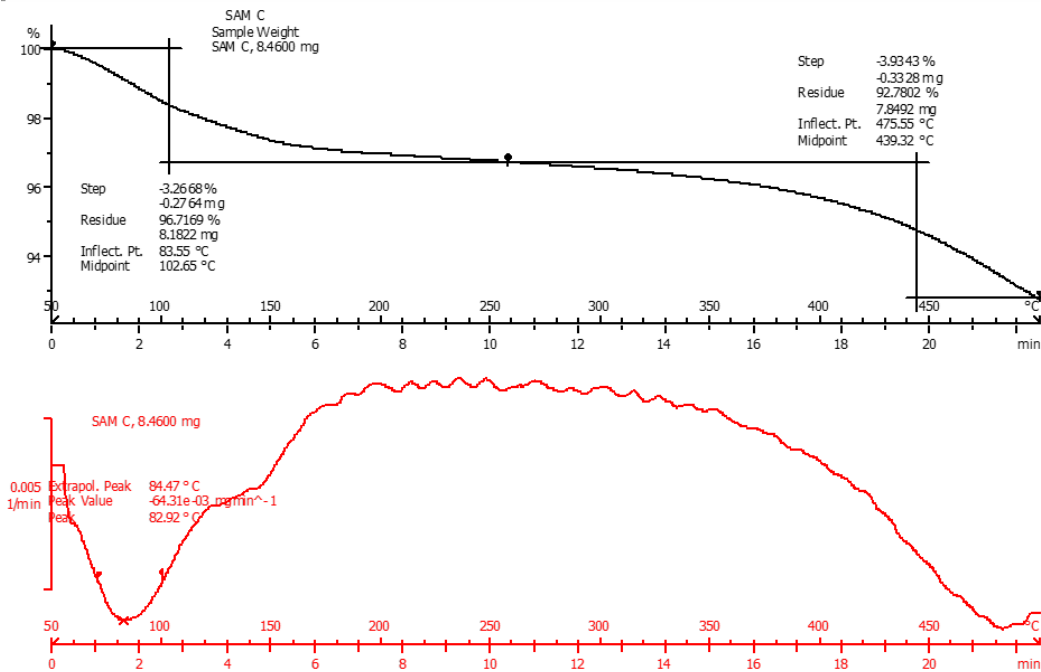


Fig. 10. Thermogram of sample C

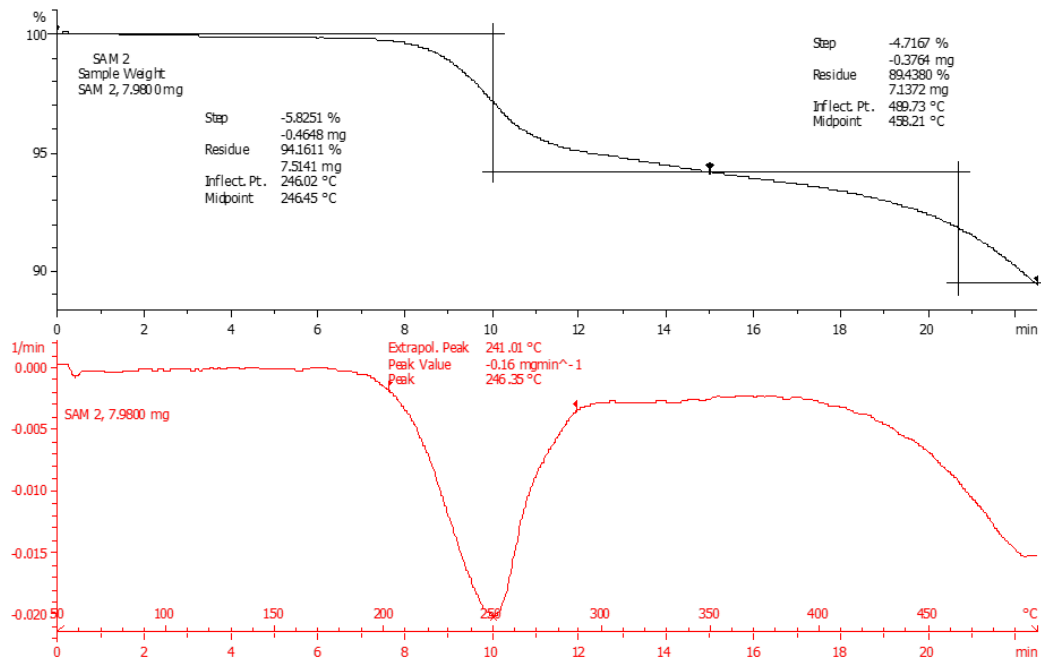


Fig. 11. Thermogram of sample 2

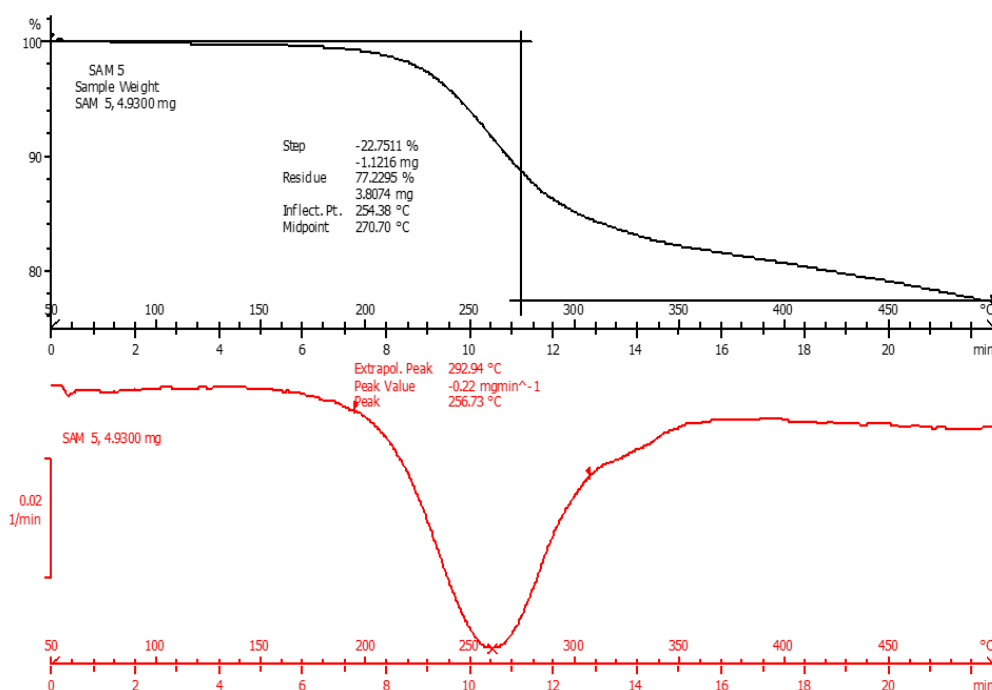


Fig. 12. Thermogram of sample 5

The second step occurred from 110°C to 200°C temperature range and is assigned to the dehydration of the hydrated cations in the interlayers of the samples [33,63]. At 200°C, the masses of Samples A, C, 2 and 5 were observed to have been reduced by about 0.5% (0.00 mg), 3.0% (0.25 mg), 0.5% (0.04 mg) and 1.0% (0.05 mg) respectively. The DTG scans in Sample A continued fluctuating as the temperature increased while that of Sample C showed a continual increase at 0.64 mg/min. The organoclay samples did not show any clear change in the DTG profile as the temperature increased in the second step. This indicated an improvement in the thermal stability and hydrophobicity of the modified materials. The proof of hydrophobicity is reflected in the thermal stability of the organoclay samples within the first 200°C on the DTG scans.

The third mass loss step occurred within the temperature range of 200°C and 350°C and explains desorption and decomposition of organic molecules from the surface of the samples. Samples A and C were reduced from their initial masses by a total of 0.3% (0.01 mg) and 3.8% (0.32 mg). The DTG profile of the Samples A and C showed relatively stable but fluctuating patterns in this step. In the organoclay samples, this step corresponded to the chemical decomposition of the bonded structure of the

organic modifier and indicated the extent of intercalation as a percentage of the modifier present in the materials. This explains two types of bonding of surfactant molecules in the organoclays. One type of bonding is to the silica surface and the second to other surfactant molecules. Sample 2 was reduced by 5.5% (0.44 mg) and Sample 5 by 18.0% (0.89 mg). The DTG profiles of Fig. 10 and Fig. 11 show an inflection from stability at 200°C which was the onset of the decomposition of the organic matter with the maximum decomposition around 250°C – 275°C, which was close to the melting point (253°C) of HDTMAB.

The final mass loss step occurred within the temperature range of 350°C - 500°C and is attributed to the loss of structural hydroxyl groups from within the clay. The thermogram of the samples showed a continuous decrease 350°C to 500°C for all the samples. At 500°C the samples had reduced totally by 1.72%, 7.2%, 10.5% and 22.8% for the Samples A, C, 2 and 5 respectively.

4. CONCLUSION

Raw clay materials with low smectite contents and varying compositions of impurities have been effectively modified into more organophilic, thermally stable and functional organoclays

materials by hydrothermal cation exchange with HDTMA⁺ for the purpose of nano-hybrid precursors and sorbents for environmental remediation. The HDTMA-exchanged clay materials showed not only morphological features such as decreased specific surface area and the irregular, wavy surface with curled edges but also structural features such as larger d-values and lattice distortion. The XRD results proved that an increase in the smectite interlayer space of the materials as a result of the intercalated HDTMA cations and that the HDTMA arrangement strongly depended on the duration of intercalation and on the packing density of surfactant within the clay galleries. This can facilitate the entry of the host organic molecules into the clay mineral interlayer space in further applications. The thermograms have revealed that these materials can be changed from being hydrophilic to hydrophobic, which is also a characteristic of successfully intercalated smectites. The intercalated structures thus formed have better heat stabilities. The selective modification of the smectites present in the clay mixture, therefore, influenced a change in the overall morphological and structural characteristics of the materials. These findings are important and vital to the preparation of low-cost and biodegradable organoclays for industrial and environmental applications.

COMPETING INTERESTS

Authors have declared that no competing interests exist.

REFERENCES

- Sarkar B, Xi Y, Megharaj M, Krishnamurti GSR, Rajarathnam D, Naidu R. Remediation of hexavalent chromium through adsorption by bentonite based Arquad[®] 2HT-75 organoclays. *J. Hazard. Mater.* 2010;183(1-3):87–97. DOI: 10.1016/j.jhazmat.2010.06.110
- Lee SM, Tiwari D. Organo and inorgano-organo-modified clays in the remediation of aqueous solutions: An overview. *Appl. Clay Sci.* 2012;59-60:84–102. DOI: 10.1016/j.clay.2012.02.006
- Moyo F, Tandlich R, Wilhelmi BS, Balaz S. Sorption of hydrophobic organic compounds on natural sorbents and organoclays from aqueous and non-aqueous solutions: A mini-review. *Int. J. Environ. Res. Public Health.* 2014;11(5):5020–48. DOI: 10.3390/ijerph110505020
- Adebajo MO, Frost RL, Klopogge JT, Carmody O, Kokot S. Porous materials for oil spill cleanup : A review of synthesis and absorbing properties. *J. Porous Mater.* 2003;10(3):159–170.
- Liu P, Zhang L. Adsorption of dyes from aqueous solutions or suspensions with clay nano-adsorbents. *Sep. Purif. Technol.* 2007;58(1):32–39. DOI: 10.1016/j.seppur.2007.07.007
- Wang D, McLaughlin E, Pfeffer R, Lin YS. Adsorption of oils from pure liquid and oil-water emulsion on hydrophobic silica aerogels. *Sep. Purif. Technol.* 2012; 99:28–35. DOI: 10.1016/j.seppur.2012.08.001
- Di Y, Iannace S, Di Maio E, Nicolais L. Poly (lactic acid) /organoclay nanocomposites: Thermal, rheological properties and foam processing. *J. Polym. Sci. Part B Polym. Phys.* 2005;43:689–698. DOI: 10.1002/polb.20366.
- Sousa F, Ramos A, Campos L. com tensoativo não-iônico para fluidos de perfuração base orgânica (Compositions of organoclays obtained with nonionic surfactant for organic base drilling. *Cerâmica.* 2011;57:199–205.
- de Paiva LB, Morales AR, Valenzuela Díaz FR. Organoclays: Properties, preparation and applications. *Appl. Clay Sci.* 2008; 42(1-2):8–24. DOI: 10.1016/j.clay.2008.02.006
- Patel HA, Somani RS, Bajaj HC, Jasra RV. Nanoclays for polymer nanocomposites , paints, inks, greases and cosmetics formulations, drug delivery vehicle and waste water treatment. *Bull. Mater. Sci.* 2006; 29(2):133–145.
- Nasreen A. Montmorillonite. *Synlett.* 2001; 8:1341–1342.
- Gámiz B, Celis R, Hermosín MC, Cornejo J. Organoclays as soil amendments to increase the efficacy and reduce the environmental impact of the herbicide fluometuron in agricultural soils. *Journal of agricultural and food chemistry.* 2010; 58(13):7893-901.
- Konta J. Clay and man: Clay raw materials in the service of man. *Appl. Clay Sci.* 1995; (10):275–335.
- Topallar H. The adsorption isotherms of the bleaching of sun ower-seed oil. *Turkish J. Chem.* 1998;22(2):143–148.

15. Motlagh MMK, Youzbashi AA, Rigi ZA. Effect of acid activation on structural and bleaching properties of a bentonite. *Iran. J. Mater. Sci. Eng.* 2011;8(4):50–56.
16. Waheed S, Rahman S, Faiz Y, Siddique N. Neutron activation analysis of essential elements in Multani mitti clay using miniature neutron source reactor. *Appl. Radiat. Isot.* 2012;70(10):2362–2369. Doi: 10.1016/j.apradiso.2012.06.030
17. He H, Yang D, Yuan P, Shen W, Frost RL. A novel organoclay with antibacterial activity prepared from montmorillonite and Chlorhexidini Acetas. *J. Colloid Interface Sci.* 2006;297(1):235–43. DOI: 10.1016/j.jcis.2005.10.031
18. Batra M, Gotam S, Dadarwal P, Nainwani R, Sharma M. Nano-Clay as Polymer Porosity Reducer: A Review. *J. Pharm. Sci. Technol.* 2011;3(10):709–716.
19. Lebaron PC, Wang Z, Pinnavaia TJ. Polymer-layered silicate nanocomposites: An overview. *Appl. Clay Sci.* 1999;15:11–29. DOI: 10.1016/S0169-1317(99)00017-4
20. Wang K, Liang S, Deng J, Yang H, Zhang Q, Fu Q, et al. The role of clay network on macromolecular chain mobility and relaxation in isotactic polypropylene/organoclay nanocomposites. *Polymer (Guildf)*. 2006;47:7131–7144. DOI: 10.1016/j.polymer.2006.07.067
21. Boukerrou A, Duchet J, Fellahi S, Djidjelli H, Kaci M, Sautereau H. Synthesis and characterization of rubbery epoxy/organoclay hectorite nanocomposites. *eXPRESS Polym. Lett.* 2007;1(12):824–830. DOI: 10.3144/expresspolymlett.2007.114
22. Uddin F. Clays, nanoclays, and montmorillonite minerals. *Metall. Mater. Trans. A.* 2008;39(12):2804–2814. DOI: 10.1007/s11661-008-9603-5
23. Finkelman RB. Health benefits of geologic materials and geologic processes. *Int. J. Environ. Res. Public Heal.* 2006;3(4):338–342.
24. Tiwari DK, Behari J, Sen P. Application of nanoparticles in waste water treatment. *World Appl. Sci. J.* 2008;3(3):417–433.
25. Nayak PS, Singh BK. Instrumental characterization of clay by XRF, XRD and FTIR. *Indian Acad. Sci.* 2007;30(3):235–238.
26. Sulaymon PAH, Kshash JM. Removal of oil from wastewater by organoclay prepared from Iraqi bentonite. *J. Eng.* 2010;16(4):5778–5798.
27. Nwankwere ET, Gimba CE, Ndukwe GI, Isuwa AK. Modelling of the kinetic and equilibrium sorption behaviour of crude oil on HDTMAB modified nigerian nanoclays. *Int. J. Sci. Technol. Res.* 2015;4(02):106–114.
28. Zhou Q, Xi Y, He H, Frost R. Application of near infrared spectroscopy for the determination of adsorbed p-nitrophenol on HDTMA organoclay simplifications for the removal of organic pollutants from water. *Spectrochim. A Mol. Biomol. Spectrosc.* 2008;69:835–841. DOI:http://dx.doi.org/10.1016/j.saa.2007.05.03
29. Zhu R, Zhu J, Ge F, Yuan P. Regeneration of spent organoclays after the sorption of organic pollutants: A review. *J. Environ. Manage.* 2009;90(11):3212–6. DOI: 10.1016/j.jenvman.2009.06.015
30. Zhou Q, Frost RL, He H, Xi Y. Changes in the surfaces of adsorbed para-nitrophenol on HDTMA organoclay-The XRD and TG study. *J. Colloid Interface Sci.* 2007; 307(1):50–55.
31. Manocha S, Patel N, Manocha L. Development and Characterisation of Nanoclays from Indian Clays. *Def. Sci. J.* 2008;58(4):517–524. DOI:10.14429/dsj.58.1672
32. Tiwari RR, Khilar KC, Natarajan U. Synthesis and characterization of novel organo-montmorillonites. *Appl. Clay Sci.* 2006;38(3):203–208.
33. Xi Y, Martens W, He H, Frost RL. Thermogravimetric analysis of organoclays intercalated with the surfactant octadecyltrimethylammonium bromide. *J. Therm. Anal. Calorim.* 2005;81(1):91–97.
34. Pedro GL, Ticiane SV, Nicole RD. Purification of a Brazilian Smectite Clay. *Mater. Sci. Forum.* 2012;727–728:929–934. DOI: 10.4028/www.scientific.net/MSF.727-728.929
35. Ross DS, Ketterings Q. Recommended methods for determining soil cation exchange capacity. In: Recommended soil testing procedures for the Northeastern United States. 1996;75–86.
36. Mallakpour S, Dinari M. Preparation and characterization of new organoclays using natural amino acids and Cloisite Na+. *Appl. Clay Sci.* 2011;51(3):353–359. DOI: 10.1016/j.clay.2010.12.028.

37. Hoidy WH, Ahmad MB, Al-Mulla EAJ, Ibrahim NAB. Synthesis and Characterization of Organoclay from Sodium Montmorillonite and Fatty Hydroxamic Acids. *Am. J. Appl. Sci.* 2009; 6(8):1567–1572.
38. Frost R, He H, Kloprogge T, Bostrom T, Duong L, Yuan P, et al. Changes in the morphology of organoclays with HDTMA+ surfactant loading. *Appl. Clay Sci.* 2006; 31(3-4):262–271.
39. Yürüdü C, Işçi S, Ünlü C, Atici O, Ece Öl, Güngör N. Synthesis and characterization of HDA/NaMMT organoclay. *Bull. Mater. Sci.* 2005;28(6):623–628. DOI: 10.1007/BF02706353
40. Zhu J, He H, Zhu L, Wen X, Deng F. Characterization of organic phases in the interlayer of montmorillonite using FTIR and ¹³C NMR. *J. Colloid Interface Sci.* 2005;286(1):239–244.
41. Nuntiya A, Sompech S, Aukkaravittayapun S. The Effect of Surfactant Concentration on the Interlayer Structure of Organoclay. *Chiang Mai J. Sci.* 2008;35(1):199–205.
42. Carmody O, Frost R, Xi Y, Serge K. Surface characterisation of selected sorbent materials for common hydrocarbon fuels. *Surf. Sci.* 2007;601(19):2066–2076.
43. Zhu JX, Zhu LZ, Zhu RL, Tian SL, Li JW. Surface microtopography of surfactant modified montmorillonite. *Appl. Clay Sci.* 2009;45:70–75.
44. Wang TH, Hsieh CJ, Lin SM, Wu DC, Li MH, Teng SP. Effect of alkyl properties and head groups of cationic surfactants on retention of cesium by organoclays. *Environ. Sci. Technol.* 2010;44(13):5142–5147.
45. Perez-Santano A, Trujillano R, Belver C, Gil A, Vicente MA. Effect of the intercalation conditions of a montmorillonite with octadecylamine. *J. Colloid Interface Sci.* 2005;284:239–244.
46. Wang C, Juang L, Lee C, Hsu T, Lee J, Chao H. Effect of exchanged surfactant cations on the pore structure and adsorption characteristics of montmorillonite. *J. Colloid Interface Sci.* 2004;27:280.
47. Vengris T, Binkiene R, Sveikauskaite A. Nickel, copper and zinc removal from water by a modified clay sorbent. *Appl. Clay Sci.* 2001;18:183–190.
48. Caglar B, Afsin B, Tabak A, Eren E. Characterization of the cation-exchanged bentonites by XRPD, ATR, DTA/TG analyses and BET measurement. *Chem. Eng. J.* 2009;149:242–248. DOI: 10.1016/j.cej.2008.10.028.
49. Mosser C, Michot LJ, Villieras F, Romeo M. Migration of cations in copper(II); Exchanged montmorillonite and laponite upon heating. *Clays Clay Miner.* 1997; 45:789–802.
50. Auboiroux M, Melou F, Bergaya F, Touray JC. Hard and soft acid-base model applied to bivalent cation selectivity on a 2:1 clay minerals. *Clays Clay Miner.* 1998;46:546–555.
51. Nguyen VN, Nguyen TDC, Dao TP, Tran HT, Nguyen DB, Ahn DH. Synthesis of organoclays and their application for the adsorption of phenolic compounds from aqueous solution. *J. Ind. Eng. Chem.* 2013;19(2):640–644. DOI:10.1016/j.jiec.2012.09.018
52. Li Z, Jiang WT, Chen CJ, Hong H. Influence of chain lengths and loading levels on interlayer configurations of intercalated alkylammonium and their transitions in rectorite. *Langmuir.* 2010; 26(11):8289–94. DOI:10.1021/la904677s
53. Lapidés I, Yariv S, Golodnitsky D. Simultaneous DTG-TG study of montmorillonite mechanochemically treated with crystal-violet. *J. Therm. Anal.* 2002;67:99–112.
54. Xi Y, Ding Z, He H, Frost RL. Structure of organoclays an X-ray diffraction and thermogravimetric analysis study. *J. Colloid Interface Sci.* 2004;277:116–120.
55. Xi Y, Frost RL, He H, Kloprogge T, Bostrom T. Modification of Wyoming montmorillonite surfaces using a cationic surfactant. *Langmuir.* 2005;21:8675–8680.
56. Lagaly G, Gonzalez MF, Weiss A. Problems in layer-charge determination of montmorillonites. *Clay Min.* 1976;11:173–187.
57. Yilmaz N, Yapar S. Adsorption properties of tetradecyl and hexadecyl trimethylammonium bentonites. *Appl. Clay Sci.* 2004;27:223–228.
58. Van der Marel HW, Beutelspacher H. *Atlas of Infrared spectroscopy of clay minerals and their admixtures.* Amsterdam: Elsevier; 1976.
59. Oliveira GC, Mota MF, Silva MM, Rodrigues MGF, Laborde HM. Performance of natural sodium clay treated with ammonium salt in the separation of

- emulsified oil in water. Brazilian J. Pet. Gas. 2012;6(4):171–183.
DOI:10.5419/bjpg2012-0014
60. Zhu R, Zhu L. Thermodynamics of naphthalene sorption to organoclays: Role of surfactant packing density. J. Colloid Interface Sci. 2008;322(1):27–32.
DOI: 10.1016/j.jcis.2008.02.026
61. Masooleh MS, Bazgir S, Tamizifar M, Nemati A. Adsorption of petroleum hydrocarbons on organoclay. J. Appl. Chem. Res. 2010;4(14):19–23.
62. Frost R, Zhou Q, He H, Xi Y. Changes in the surfaces of adsorbed parnitrophenol on HDTMA organoclay -an XRD and TG study. J. Colloid Interface Sci. 2007; 307(1):50–55.
63. Magaraphan R, Lilayuthalert W. Preparation, structure, properties and thermal behavior of rigid-rod polyimide/MMT nanocomposites. Compos Sci. Technol. 2001;61:1253–1264.
64. Venkatathri N. Characterization and catalytic properties of naturally occurring clay, bentonite. Bull. Catal. Soc. India. 2006;5:61–72.

© 2017 Nwankwere et al.; This is an Open Access article distributed under the terms of the Creative Commons Attribution License (<http://creativecommons.org/licenses/by/4.0>), which permits unrestricted use, distribution, and reproduction in any medium, provided the original work is properly cited.

Peer-review history:
The peer review history for this paper can be accessed here:
<http://sciencedomain.org/review-history/17712>